JACS
JOURNAL OF THE AMERICAN CHEMICAL SOCIETY
Article
pubs.acs.org/JACS

Tailored Donor–Acceptor Polymers with an A–D1–A–D2 Structure: Controlling Intermolecular Interactions to Enable Enhanced Polymer Photovoltaic Devices

Tianshi Qin,*[,†] Wojciech Zajaczkowski,[‡] Wojciech Pisula,[‡] Martin Baumgarten,[‡] Ming Chen,[†] Mei Gao,[†] Gerry Wilson,[†] Christopher D. Easton,[†] Klaus Müllen,*[,‡] and Scott E. Watkins*[,†]

[†]Ian Wark Laboratory, CSIRO Materials Science & Engineering, Clayton South, Victoria 3169 Australia
[‡]Max Planck Institute for Polymer Research, Ackermannweg 10, D-55128 Mainz, Germany

Supporting Information

ABSTRACT: Extensive efforts have been made to develop novel conjugated polymers that give improved performance in organic photovoltaic devices. The use of polymers based on alternating electron-donating and electron-accepting units not only allows the frontier molecular orbitals to be tuned to maximize the open-circuit voltage of the devices but also controls the optical band gap to increase the number of photons absorbed and thus modifies the other critical device parameter—the short circuit current. In fact, varying the nonchromophoric components of a polymer is often secondary to the efforts to adjust the intermolecular aggregates and improve the charge-carrier mobility. Here, we introduce an approach to polymer synthesis that facilitates simultaneous control over both the structural and electronic properties of the polymers. Through the use of a tailored multicomponent acceptor–donor–acceptor (A–D–A) intermediate, polymers with the unique structure A–D1–A–D2 can be prepared. This approach enables variations in the donor fragment substituents such that control over both the polymer regiochemistry and solubility is possible. This control results in improved intermolecular π-stacking interactions and therefore enhanced charge-carrier mobility. Solar cells using the A–D1–A–D2 structural polymer show short-circuit current densities that are twice that of the simple, random analogue while still maintaining an identical open-circuit voltage. The key finding of this work is that polymers with an A–D1–A–D2 structure offer significant performance benefits over both regioregular and random A–D polymers. The chemical synthesis approach that enables the preparation of A–D1–A–D2 polymers therefore represents a promising new route to materials for high-efficiency organic photovoltaic devices.

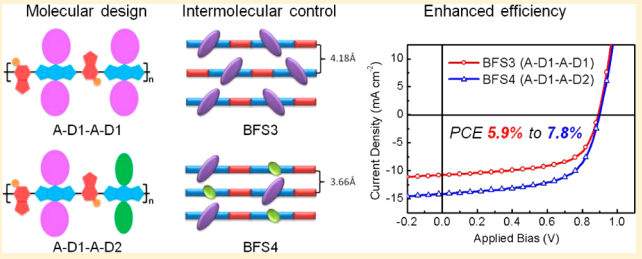

INTRODUCTION

Bulk heterojunction (BHJ) organic photovoltaics (OPVs), based on blends of conjugated polymers and soluble fullerene derivatives, have attracted attention due to their unique advantages of solution processability, flexibility, lightweight, large area, and low cost production.[1] Over the past few years, organic chemists and material scientists have been working toward developing novel molecular structures and device architectures to improve the performance of photovoltaic devices.[2] To maximize the performance of OPV devices,[3] attention has shifted beyond just the molecular formula to other considerations such as molecular weight characteristics,[4] chemical and thermal stabilities,[5] end-group contributions,[6] and extrinsic impurities[7] as well as intra- and intermolecular charge carrier mobilities.[8] In addition, strategies such as the use of annealing processes or additives[9] as well as the use of interfacial materials[10] have been employed.

Progress due to advances in the chemical structure of materials has mainly come through the use of a donor–acceptor (D–A) approach; polymers based on alternating fragments of electron-rich and electron-poor groups. This combination allows the molecular orbitals to be tuned so as to enable intramolecular charge transfer (ICT).[11] The open circuit voltage (V_{oc}) of OPVs is directly related to the gap between the highest occupied molecular orbital (HOMO) of the polymer and lowest unoccupied molecular orbital (LUMO) of the fullerene. Tuning of the polymer molecular orbitals therefore enables the V_{oc} to be maximized. While straightforward in design and practice, the use of simple, D–A polymers has a number of drawbacks. First, conventional polycondensation polymerizations do not allow regioselectivity when asymmetric monomers are employed. As such, there is no control over the orientation of functional groups with respect to each other. Regioregular polymers have a regular, alternating structure, whereas random polymers have substituents that are randomly oriented along the chain. It is well-known that variations in molecular order reduce intermolecular π-stacking interactions that in turn can limit charge transport through polymer films.[12] A second disadvantage of simple D–A polymers is that there

Received: February 2, 2014
Published: April 4, 2014

   dx.doi.org/10.1021/ja500935d | J. Am. Chem. Soc. 2014, 136, 6049–6055

are only two variables, the solubilizing groups on the acceptor and donor fragments. This means that the solubility of the polymer can only be altered by changing all of the solubilizing groups on a donor or acceptor fragment at once. Such a change could dramatically alter the properties of the polymer. A recent perspective article emphasized how the size and topology of side chains as well as the orientation of repeating units can influence the macroscopic properties of polymers.[13]

The design strategy conceived in this work is illustrated in Scheme 1. We present a stepwise synthetic strategy, based on an intermediate A−D−A intermediate, which provides simultaneous control over both the polymer regiochemistry and solubility. In this terminology, "A" represents an electron-accepting group, and "D" represents an electron-donating group. This route provides access to a series of π-conjugated polymers based on both A−D1−A−D1 and A−D1−A−D2 structures. In the latter, two different donor fragments (D1 and D2) are used, and the structure of the polymer is controlled. In side-by-side comparisons we demonstrate that by controlling the orientation of substituents and the amount of non-chromophoric components in the polymer, the macromolecular interactions can be enhanced which in turn lead to significant improvements in the short-circuit current densities of the OPVs.

Scheme 1. Design Strategy Based on an A−D−A Intermediate[a]

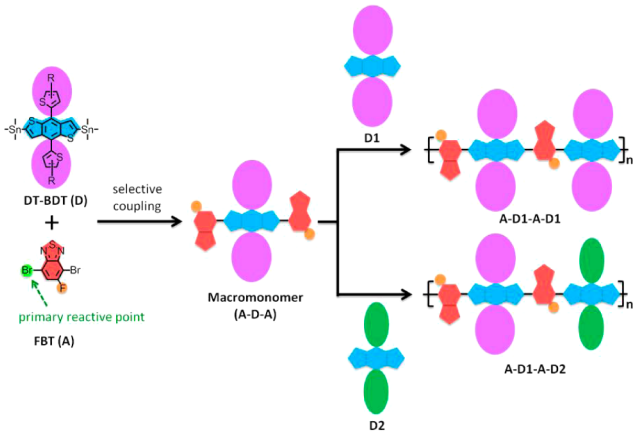

[a]The different coloured ellipses on D1 and D2 represent different substituents.

As outlined above, our strategy enables two different donor fragments to be used while still maintaining an alternating D−A structure. Janssen et al. have recently shown that combining the properties of multiple D−A copolymer systems can have advantageous benefits.[14] Patil et al. have described an A1−D−A2−D polymer for use in OFETs where optimized chain packing and the formation of large crystalline domains in the solid state dramatically enhanced charge-carrier mobility.[15] Our design strategy is distinct in that it extends on these ideas by also providing a means to control the regiochemistry of the polymer through the fixed orientation of the acceptor fragments. To demonstrate the strategy we sought donor and acceptor fragments that would (i) enable variation in the positioning of side chains and (ii) enable controllable reactivity in an asymmetric monomer. After a review of the literature dithienyl-benzo[1,2-b:4,5-b′]dithiophene (**DT-BDT**)[16] and 5-fluoro-2,1,3-benzothiadiazole (**FBT**)[17] were selected as they could satisfy both requirements. Compared with other well-known donor units, such as silafluorene[18] or dithienosilole,[19] in which two out-of-plane side chains have to be located on the fused heteroatom between the aromatic rings, the **DT-BDT** unit can provide multiple positions for solubilizing substituents with varied out-of-plane dihedral angles. For the acceptor fragment, monofluoro substituted benzothiadiazole (**FBT**) is one of only two reported acceptor units (the other is pyridalthiadiazole[20]), which demonstrates asymmetric reactivity between ortho- and meta-positions.

RESULTS AND DISCUSSION

Synthesis. To begin, we prepared two **DT-BDT** monomers (**D1** and **D2**, Figure S3) as donor units with various substituted alkyl-chains as well as the acceptor monomer 3,6-dibromo-5-fluoro-2,1,3-benzothiadiazole (**FBT**) (**A**, Figure S3). By using direct or stepwise synthesis methods, four novel **DT-BDT-FBT** based conjugated polymers with either random (**BFR1** and **BFR2**) or regioregular (**BFS3** and **BFS4**) orientations in the polymer backbone were achieved, Scheme 2. The random and regioregular labels refer to the orientation of the fluorine atom on the **FBT** fragment with respect to the donor fragment. The synthetic routes are shown in Figure S3. The branched 2-ethylhexyl chain was first used on the **DTBDT** units in an attempt to ensure adequate solubility of the target polymers. Unfortunately, the first random copolymer **BFR1** demonstrated limited solubility and could not be processed using common solvents. Accordingly, an extra linear hexyl chain was added to the design, resulting in the second random copolymer **BFR2** with high solubility in chloroform, chlorobenzene and dichlorobenzene. Polymer **BFR2** is a control for comparison with the regioregular polymers **BFS3** and **BFS4**.

Scheme 2. Repeat Units of the DT-BDT-FBT-Based Polymers[a]

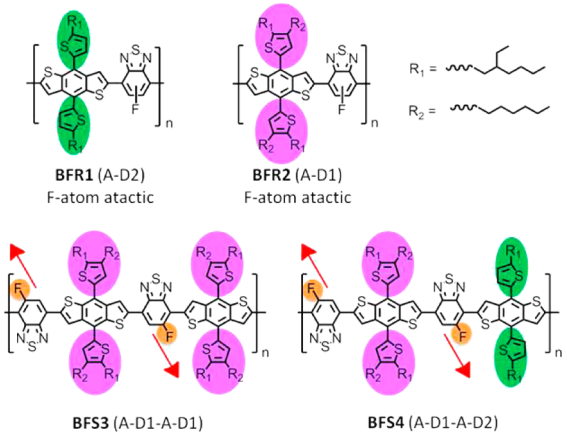

[a] Random F-atom arranged **BFR1** and **BFR2**, regioregular **BFS3** and **BFS4**. The coloured ellipses highlight the different solubilising groups, and the red arrows emphasize the regiochemical control.

Polymers **BFS3** and **BFS4** were prepared in a two-step route via an **A−D1−A** intermediate. Control over the structure of the intermediate was achieved due to the preferential reaction of the Pd-catalyzed Stille coupling at the position meta- to the fluorine atom on the **FBT** group. This asymmetric reactivity gave the **A−D1−A** intermediate in yields as high as 90%. The proposed regiochemical structure was confirmed by 2D NMR spectroscopy (Figure S4). No proton peaks were observed

dx.doi.org/10.1021/ja500935d | J. Am. Chem. Soc. 2014, 136, 6049−6055

from A or D1 starting materials or from their polymeric side product. The **A−D1−A** intermediate was then used to prepare the two regioregular, conjugated polymers **BFS3** and **BFS4**. Coupling **A−D1−A** with monomer **D1** and **D2**, respectively, varied the amounts of pendant side chains while keeping the basic conjugated polymer backbone unchanged. **BFR2** and **BFS3** are structural isomers differing only in the fact that in the latter the position of the fluorine atom is controlled, while in the former it is random. Polymer **BFS4** has a lower proportion of nonchromophoric groups while still maintaining high solubility in common solvents.

Thermal, Optical, and Optoelectrical Properties. High-temperature gel permeation chromatography (HT-GPC) was employed to evaluate the molecular weight distribution of the conjugated polymers. Although the random polymer **BFR1** showed poor solubility and could not be analyzed, the other three polymers were soluble in 1,2,4-trichlorobenzene which is used as the eluent in the HT-GPC system. The regioregular polymer **BFS4** was prepared with a high molecular weight with M_n = 46 kDa and PDI = 2.8. For comparison, batches of the two regioregular polymers **BFS3** and **BFS4** were synthesized with similar molecular weights and polydispersity as the random counterpart **BFR2** (Figure S5).

The molar extinction coefficients of the three, soluble, conjugated polymers in chloroform solutions with a concentration of 10^{-6} M and the absolute absorbance spectra of neat, 100 nm thick films are shown in Figure 1, and the data listed in Table 1. In dilute solutions, the main absorption band of polymer **BFS4** is bathochromically shifted and broadened to some extent in comparison to that of its analogue **BFS3** and random counterpart **BFR2**. This difference can be attributed to enhanced intermolecular $\pi-\pi$ interactions resulting from the reduced size of the pendant side groups and the regioregular arrangement of the polymer main chain.[21] In the solid-state absorption spectra these differences were even more pronounced. The maximum absorption edge of **BFR2** and **BFS3** was at 778 and 783 nm, respectively, and 793 nm for **BFS4**. Furthermore, the absorption intensity of **BFS4** as a thin film was higher than the other two polymers, an observation that is consistent with the reduction of the proportion of nonchromophoric alkyl chains in the polymer.[22] The onset of the film absorbance spectra was used to estimate the HOMO−LUMO gaps of the three polymers, **BFR2**, **BFS3**, and **BFS4**. Photoelectron spectroscopy in air (PESA) was applied to estimate the HOMO of these conjugated polymers in thin films (Figure S6).[23] The experimentally determined HOMO values and the calculated LUMO levels are summarized in Table 1. It is clear that the variations to the polymers described here do not have a significant effect on the energy levels of the materials.

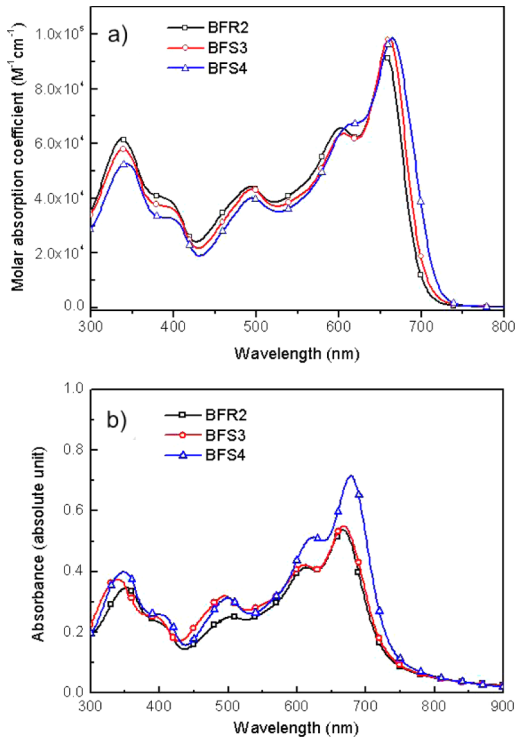

Figure 1. UV−vis absorption spectra of DT-BDT-FBT polymers. (a) Molar absorptivities (ε) of **BFR2** (□), **BFS3** (○), and **BFS4** (△) in 10^{-6} M chloroform solutions. (b) Absolute absorbance spectra of the corresponding polymers in 100 nm films.

Table 1. Optical, Optoelectronic, And Frontier Molecular Orbital Level Data

	solution[a]		film[b]				
polymer	λ_{max} (nm)	λ_{edge} (nm)	λ_{max} (nm)	λ_{edge} (nm)	E_g^{opt}(eV)[c]	HOMO (eV)[d]	LUMO (eV)
BFR2	656	733	667	778	1.59	5.20	3.61
BFS3	661	744	668	783	1.58	5.20	3.62
BFS4	665	749	678	793	1.56	5.15	3.59

[a]10^{-6} M in chloroform solution. [b]100 nm thick film. [c]Calculated from λ_{edge} of film. [d]Estimated by PESA.

Intermolecular Interactions. The organization of the regioregular polymers **BFR2**, **BFS3**, and **BFS4** in the bulk solid state was investigated by using two-dimensional, wide-angle X-ray scattering (2D-WAXS) measurements (Figure 2a−c).[24]

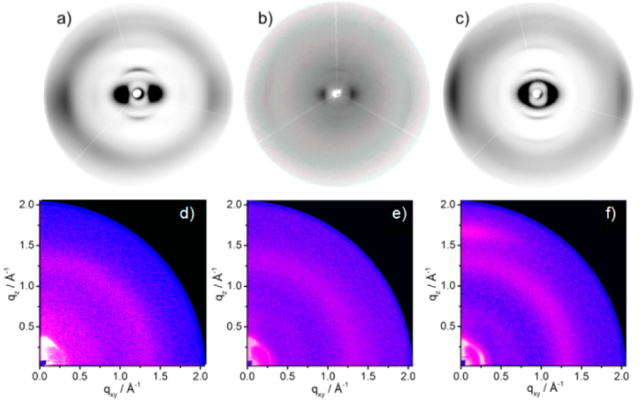

Figure 2. 2D-WAXS patterns of filament extruded polymers of (a) **BFR2**, (b) **BFS3**, and (c) **BFS4** at 30 °C and GIWAXS patterns of (d) **BFR2**/$PC_{61}BM$, (e) **BFS3**/$PC_{61}BM$, and (f) **BFS4**/$PC_{61}BM$ thin films.

Fibers of the neat polymers were macroscopically aligned by extrusion, and no further thermal pre- or postannealing processes were applied in order to ensure the same thermal treatment as during the device fabrication. At 30 °C the polymers revealed a characteristic pattern with reflections being distributed in the equatorial and meridional planes.[25] However, significant differences in intensity and position of the reflections were evident for both systems. The positions of the reflections of **BFR2** and **BFS3** in the equatorial small- and wide-angle

dx.doi.org/10.1021/ja500935d | J. Am. Chem. Soc. 2014, 136, 6049−6055

region are similar (Figures 2a,b and S7). However, **BFS3** displayed only a faint 2D pattern due to its poor scattering. For both polymers, the equatorial small-angle reflections were attributed to a chain-to-chain distance of 19.65 Å between the lamellar structures; the broad wide-angle scattering intensity on the same plane was ascribed to a quite large stacking distance of 4.18 Å, and the meridional, middle-angle position scattering reflection, corresponding to a *d*-spacing of 12.0 Å for **BFR2** and 12.65 Å for **BFS3**, was assigned to the length of the single DT-BDT repeat unit of polymer chain.[19] By contrast, **BFS4** exhibited sharper, more distinct and a higher number of reflections with a chain-to-chain distance of 24.51 Å, much smaller stacking distance of 3.66 Å and an unchanged repeating spacing between DT-BDT units of 12.8 Å (Figures 2c and S7). Thus, the significantly closer packing and higher crystallinity for **BFS4** in the bulk are in agreement with the absorption data and could be related to the polymer structure.

To gain further information about the organization in the solar cell, grazing incidence WAXS (GIWAXS) on thin films was performed (Figure 2d–f). The thin films were prepared in the same way as for the devices including the PEDOT:PSS surface and the blending with $PC_{61}BM$ and 1,8-diiodooctane. In both cases, the order was lower than in the bulk as indicated by the lack of higher order reflections. This could be attributed to the spin-coating process. Nevertheless, a significant distinction in surface organization between the polymers could be derived. The meridional position of the wide-angle scattering intensity at q_{xy} = 0 $Å^{-1}$ and q_z = 1.72 $Å^{-1}$ in the pattern for **BFS4** (Figures 2f and S8), which was related to the stacking distance of 3.66 Å, was characteristic for a face-on arrangement of the backbones toward the surface. In accordance with this alignment, the chain-to-chain reflections appeared in the small-angle equatorial plane. Additional meridional small-angle reflections were due to an edge-on orientation of a certain misaligned polymer fraction leading to a mixed organization with a coexistent face- and edge-on arrangement in the film.[26] It is expected that a face-on polymer arrangement favors the charge carrier transport perpendicular to the surface as is the case in a solar cell. By contrast, **BFR2** and **BFS3** reveal only a meridional small-angle scattering intensity and no π-stacking reflection indicating low order in edge-on arranged polymer lamellae (Figures 2d,e and S8). Therefore, with respect to both factors, better packing and face-on orientation, the data suggest that **BFS4** is more optimized for solar cell applications than **BFS3**.

Computational analysis of the **D–A** dimer fragment in the two regioregular polymers (**BFS3** and **BFS4**) by density functional theory (DFT)[27] at the B3LYP/6-31+G(d,p) level of theory estimated that the dihedral angle between donor and acceptor units is only 5–7°, meaning that the polymer backbones should be planar (Figure 3a). The pendant thiophene unit on the **BDT** unit displayed a calculated dihedral angle around 51–55°. This means that the alkyl substituents may hinder close packing of the polymer chains. We then used a semiempirical AM1 method[28] to calculate the volume of space occupied by the various alkyl chains. For the bis-substituted donor fragment the combination of the para-substituted ethylhexyl and meta-substituted hexyl chains occupies a sphere with a maximum diameter of 4.8 Å (Figure 3b). By contrast, for the monosubstituted donor fragment, with only a single para-substituted ethylhexyl group, the maximum size of a sphere occupied by the alkyl chains is significantly smaller, around 2.2 Å. As noted previously, the 2D-WAXS

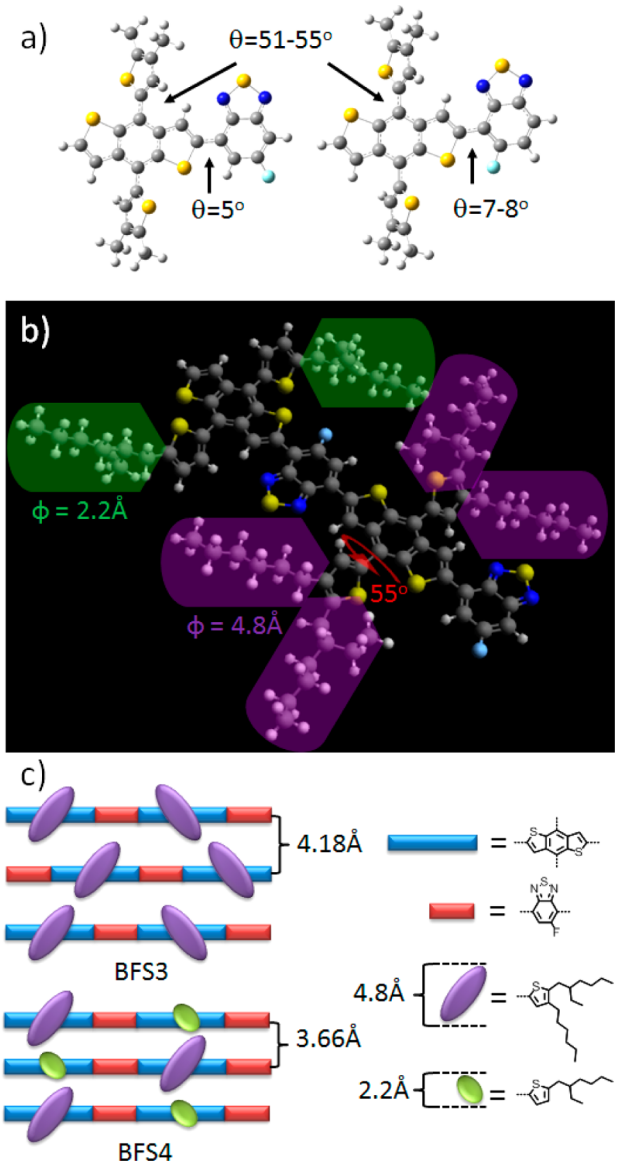

Figure 3. Computational representations. (a) B3LYP/6-31+G(d,p) calculation of D–A dimer fragments. (b) 3D simulation (semi-empirical AM1 model) of repeating unit A–D1–A–D2 in **BFS4**. (c) Schematic edge-view illustration of the possible supramolecular organization in **BFS3** and **BFS4**.

analysis showed that stacking distance reduced by around 0.52 Å from 4.18 Å for **BFS3** to 3.66 Å for **BFS4** for unannealed bulk organization. For **BFS3**, every donor fragment features the large (4.8 Å) bis-substituted group. Two adjacent bis-substituted groups when aligned directly would fill a space that is larger than the measured π–π stacking distance. It is therefore likely that, in **BFS3**, the donor fragments in adjacent chains are offset with respect to each other (Figure 3c). By contrast, the presence of the smaller, monosubstituted donor fragment in **BFS4** should not hinder the close approach of donor units on adjacent chains as the sum of the calculated maximum distance occupied by a large and small donor unit [(4.8 + 2.2 Å)/2] = 3.5 Å is less than the measured stacking distance of 3.66 Å. It has previously been shown that D–A polymers are known to prefer an arrangement, where D and A groups on adjacent chains align with the same groups above and below in a columnar fashion.[29] By reducing the steric bulk

dx.doi.org/10.1021/ja500935d | J. Am. Chem. Soc. 2014, 136, 6049–6055

of the substituents in **BFS4** we postulate that an arrangement closer to an aligned, columnar structure (Figure 3c) is possible and is indeed consistent with the WAXS data. Such an outcome is directly attributable to the structural control provided by our synthetic method.

Device Performances. In order to investigate the influence of the intermolecular interactions of the conjugated polymers on their electronic properties, single charge carrier devices were prepared. The measured current density/voltage ($J-V$) characteristics were then fitted by using the space-charge-limited current (SCLC) model.[30] At a typical electric field of 10^5 V cm^{-1} (corresponding to an applied voltage of 1 V to a 100 nm neat polymer device), the observed occurrence of a SCLC enabled a direct estimate of the hole mobility of 2.3×10^{-5}, 2.0×10^{-4}, and 1.5×10^{-3} cm^2 V^{-1} s^{-1} for **BFR2**, **BFS3**, and **BFS4**, respectively (Figure S9). At a high voltage of 5 V, **BFS4** also exhibited a field-dependent electron mobility[31] of 7.5×10^{-4} cm^2 V^{-1} s^{-1} (at 5×10^5 V cm^{-1}, Figure S10). Notably, neither of the other two polymers showed any measurable electron mobility. The observation that **BFS4** has both the highest hole mobility and a measurable electron mobility is consistent with the highest order and close π-stacking distance as derived from the structural analysis, and the structure postulated above whereby the reduced steric bulk permits an arrangement that is closer to a columnar structure. The high charge mobility for **BFS4** is also desirable with respect to increasing the short circuit current density (J_{SC}) in OPV devices.

OPV devices were fabricated using these three polymers (**BFR2**, **BFS3**, and **BFS4**), in turn, as the electron donor and $PC_{61}BM$ as the electron acceptor. The device structure was ITO/PEDOT:PSS/polymer:$PC_{61}BM$/PFN/Al. PFN is a polyelectrolyte that is used as an interlayer to assist with charge extraction.[32] The optimized weight ratio of polymer to $PC_{61}BM$ is 1:1.4. About 2% (1,8-diiodooctane (DIO)/*o*-dichlorobenzene (*o*-DCB), v/v) of DIO was added as an additive to enable differential solubility.[33] No thermal pre- or postannealing processes were applied during the device fabrication. Device $J-V$ characteristics are shown in Figure 4a, and the parameters are listed in Table 2. From the $J-V$ curves, a clear improvement of photovoltaic properties was observed in going from the random to the regioregular polymers. The V_{OC} and fill factor (FF) values were in the same range for the three polymers, a finding that is consistent with their similar HOMO levels, equal D/A ratio, and identical device structures. However, the J_{SC} values for devices based on **BFS4** were significantly increased in comparison with those of **BFS3** and **BFR2**, even with similar molecular weights. Notably, a J_{SC} as high as 14.20 mA/cm^2 was obtained for devices based on **BFS4** and $PC_{61}BM$. Combined with its high V_{OC} and FF, a high PCE of 7.38 ± 0.4% (average from 40 devices, simulated sunlight, AM 1.5G, 100 mW cm^{-2}) was achieved, the highest measured PCE being 7.80%. To the best of our knowledge, the only reports of higher PCEs from polymer OPV devices make use of the higher cost C_{70} derivative.

To further explore the properties of the devices, the incident photon-to-current efficiency (IPCE) of the devices based on the three polymers was measured. The IPCE curves are shown in Figure 4b. All the devices exhibited a good response to short-wavelength sunlight in the range 300–450 nm, attributable to the contribution of $PC_{61}BM$.[34] Their photo conversion efficiencies in the long-wavelength range, 450–750 nm, which correspond to the absorption of the polymers,[35] varied from

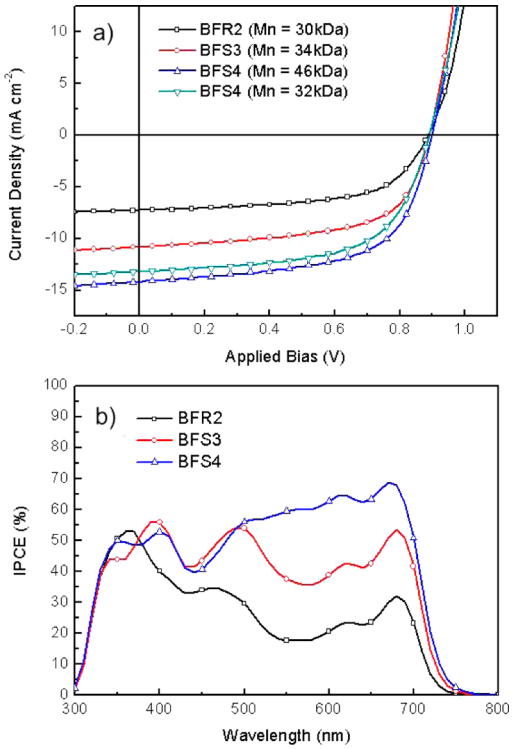

Figure 4. OPV performance of DT-BDT-FBT polymers. (a) Photocurrent density–voltage ($J-V$) curves of **BFR2** (□), **BFS3** (○) and **BFS4** (△) under illumination of AM 1.5G, 100 mW cm^{-2}. (b) IPCE curves of the corresponding OPVs.

Table 2. Photovoltaic Properties of the OPVs Based on DT-BDT-FBT Polymers/$PC_{61}BM$

						PCE (%)	
polymer	M_n (kDa)	PDI	V_{OC} (V)	J_{SC} (mA/cm^2)	FF (%)	best	ave[a]
BFR2	30	2.2	0.89	−7.25	60.56	3.91	3.74
BFS3	34	2.2	0.90	−10.82	60.81	5.92	5.67
BFS4	32	2.3	0.90	−13.19	60.33	7.16	7.02
BFS4[b]	46	2.8	0.90	−14.20	61.05	7.80	7.38

[a]Averaged from at least 40 devices. [b]Results are shown for two different batches of **BFS4**.

17–32% to 36–54% and up to 60–68% for **BFR2**, **BFS3**, and **BFS4**, respectively. The integrated IPCE curves give calculated J_{sc}s of 7.5, 10.7, and 14.0 mA/cm^2 for **BFR2**, **BFS3**, and **BFS4**, respectively, confirming the accuracy of our photovoltaic measurements. These results are again consistent with the conclusion that the increased structural order and a reduction in the proportion of nonchromophoric side chains are responsible for the significant improvements in device performance.

The advantageous effect of the A–D1–A–D2 structure on the PCE is most likely also related to the microstructure of the bulk heterojunction blends that are obtained during film deposition. AFM phase images of the photoactive layers reveal clear phase separation arising from aggregated polymer chains (Figure 5). **BFR2**/$PC_{61}BM$ and **BFS3**/$PC_{61}BM$ phase images are dominated by areas of dark phase (i.e., a low phase value), with needle-shaped bright phase regions ranging in length from approximately 10 to 200 nm. For **BFS4**/$PC_{61}BM$, the needle-shaped regions are more densely packed, leading to larger

dx.doi.org/10.1021/ja500935d | J. Am. Chem. Soc. 2014, 136, 6049–6055

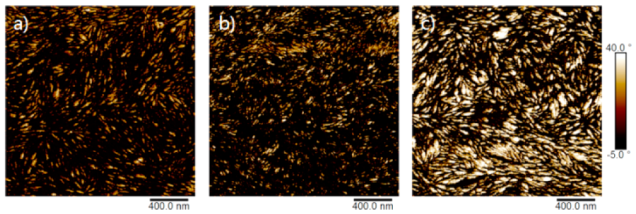

Figure 5. AFM phase images of the photoactive layers: (a) **BFR2**/$PC_{61}BM$, (b) **BFS3**/$PC_{61}BM$, and (c) **BFS4**/$PC_{61}BM$ thin films.

islands of bright phase and a greater ratio of bright to dark phase for this blend. Thus, the bright phases mostly likely correspond to the donor material as we expect closer packing for **BFS4**. The superior device performance of **BFS4** is therefore likely the result of the packing density and frequency of these regions observed herein.

CONCLUSION

To conclude, we have demonstrated a chemical design approach to improving the performance of organic solar cells. The J_{SC} of the OPV devices was increased through the use of tailored A−D−A intermediates and a stepwise approach to the synthesis of conjugated polymers. We have shown that the use of A−D1−A−D2 repeating units, as opposed to a typical A−D structure, enables control of the supramolecular interactions within a polymer film. Specifically, our method enables control over both the regiochemistry of the polymer backbone and the amount of nonchromophoric components in the polymer. Through molecular simulations backed by 2D-GIWAXS measurements we have presented compelling evidence that the intermolecular π-stacking interactions have been enhanced. In turn, these conclusions were supported by AFM, charge mobility, and photovoltaic device measurements that show significant improvements in the performance of the OPVs. Using the **BFS4** polymer in a BHJ OPV with $PC_{61}BM$ a PCE higher than 7% has been reported. More generally, the approach we have presented also provides an opportunity to further vary the optoelectronic properties of conjugated polymers through the use of two different electron-donor units. For example, the synthesis of A−D1−A−D2 type structures is now possible where D1 and D2 are electronically and not just structurally different. Such work would also enable a focus on increasing the V_{OC} and therefore even further improve device performance.

ASSOCIATED CONTENT

Supporting Information

Experimental details of synthesis and additional characterization; figures and tables as described in the text; description of the material included. This material is available free of charge via the Internet at http://pubs.acs.org.

AUTHOR INFORMATION

Corresponding Authors

tianshi.qin@csiro.au
scott.watkins@csiro.au
muellen@mpip-mainz.mpg.de

Notes

The authors declare no competing financial interest.

ACKNOWLEDGMENTS

This research was funded through the Flexible Electronics Theme of the CSIRO Future Manufacturing Flagship and was also supported by the Victorian Organic Solar Cell Consortium (Victorian Department of Primary Industries, Victorian Department of Business and Innovation and the Australian Renewable Energy Agency (ARENA)) and the Australian Centre for Advanced Photovoltaics (ACAP). W.P., M.B., and K.M. acknowledge financial support from the ERC grant NANOGRAPH, European Community EC-ITN-SUPERIOR (GA-2009-238177) and the Nano Sci-E SENSORS program. T.Q. acknowledges a Postdoctoral Fellowship from the CSIRO Office of the Chief Executive and a Postdoctoral Fellowship from ARENA. T.Q. thanks Dr. Xiwen Chen for supply of the interfacial PFN material, Dr. Noel W. Duffy for IPCE data collection, and Dr. Roger Mulder for 2D-NMR measurements.

REFERENCES

(1) Li, G.; Zhu, R.; Yang, Y. *Nat. Photonics* **2012**, *6*, 153−161.
(2) (a) Li, Y. F. *Acc. Chem. Res.* **2012**, *45*, 723−733. (b) Sun, Y. M.; Welch, G. C.; Leong, W. L.; Takacs, C. J.; Bazan, G. C.; Heeger, A. J. *Nat. Mater.* **2012**, *11*, 44−48. (c) He, Z. C.; Zhong, C. M.; Su, S. J.; Xu, M.; Wu, H. B.; Cao, Y. *Nat. Photonics* **2012**, *6*, 591−595. (d) Dou, L. T.; You, J. B.; Yang, J.; Chen, C. C.; He, Y. J.; Murase, S.; Moriarty, T.; Emery, K.; Li, G.; Yang, Y. *Nat. Photonics* **2012**, *6*, 180−185.
(3) Janssen, R. A. J.; Nelson, J. *Adv. Mater.* **2013**, *25*, 1847−1858.
(4) Chu, T. Y.; Lu, J. P.; Beaupre, S.; Zhang, Y. G.; Pouliot, J. R.; Zhou, J. Y.; Najari, A.; Leclerc, M.; Tao, Y. *Adv. Funct. Mater.* **2012**, *22*, 2345−2351.
(5) Jorgensen, M.; Norrman, K.; Gevorgyan, S. A.; Tromholt, T.; Andreasen, B.; Krebs, F. C. *Adv. Mater.* **2012**, *24*, 580−612.
(6) Park, J. K.; Jo, J.; Seo, J. H.; Moon, J. S.; Park, Y. D.; Lee, K.; Heeger, A. J.; Bazan, G. C. *Adv. Mater.* **2011**, *23*, 2430−2435.
(7) Ashraf, R. S.; Schroeder, B. C.; Bronstein, H. A.; Huang, Z. G.; Thomas, S.; Kline, R. J.; Brabec, C. J.; Rannou, P.; Anthopoulos, T. D.; Durrant, J. R.; McCulloch, I. *Adv. Mater.* **2013**, *25*, 2029−2034.
(8) Johnson, K.; Huang, Y. S.; Huettner, S.; Sommer, M.; Brinkmann, M.; Mulherin, R.; Niedzialek, D.; Beljonne, D.; Clark, J.; Huck, W. T. S.; Friend, R. H. *J. Am. Chem. Soc.* **2013**, *135*, 5074−5083.
(9) (a) Chen, L. M.; Hong, Z. R.; Li, G.; Yang, Y. *Adv. Mater.* **2009**, *21*, 1434−1449. (b) Peet, J.; Kim, J. Y.; Coates, N. E.; Ma, W. L.; Moses, D.; Heeger, A. J.; Bazan, G. C. *Nat. Mater.* **2007**, *6*, 497−500.
(10) (a) Tan, Z. A.; Zhang, W. Q.; Zhang, Z. G.; Qian, D. P.; Huang, Y.; Hou, J. H.; Li, Y. F. *Adv. Mater.* **2012**, *24*, 1476−1481. (b) He, Z. C.; Zhong, C. M.; Huang, X.; Wong, W. Y.; Wu, H. B.; Chen, L. W.; Su, S. J.; Cao, Y. *Adv. Mater.* **2011**, *23*, 4636−4643.
(11) Li, Y. W.; Guo, Q.; Li, Z. F.; Pei, J. N.; Tian, W. J. *Energy Environ. Sci.* **2010**, *3*, 1427−1436.
(12) (a) Kim, Y.; Cook, S.; Tuladhar, S. M.; Choulis, S. A.; Nelson, J. *Nat. Mater.* **2006**, *5*, 197−203. (b) Li, G.; Shrotriya, V.; Huang, J. S.; Yao, Y.; Moriarty, T.; Emery, K.; Yang, Y. *Nat. Mater.* **2005**, *4*, 864−868.
(13) (a) Piliego, C.; Holcombe, T. W.; Douglas, J. D.; Woo, C. H.; Beaujuge, P. M.; Fréchet, J. M. J. *J. Am. Chem. Soc.* **2010**, *132*, 7595−7597. (b) Rivnay1, J.; Toney, M. F.; Zheng, Y.; Kauvar, I. V.; Chen, Z. H.; Wagner, V.; Facchetti, A.; Salleo, A. *Adv. Mater.* **2010**, *22*, 4359−4363. (c) Mei, J. G.; Kim, D. H.; Ayzner, A. L.; Toney, M. F.; Bao, Z. H. *J. Am. Chem. Soc.* **2011**, *133*, 20130−20133. (d) Beaujuge, P. M. Fréchet, J. M. J. *J. Am. Chem. Soc. 133*, 20009−20029. (e) Mei, J. G.; Bao, Z. N. *Chem. Mater.* **2013**, *26*, 604−615. (f) Henson, Z. B.; Müllen, K.; Bazan, G. C. *Nat. Chem.* **2012**, *4*, 699−704.
(14) Hendriks, K. H.; Heintges, G. H. L.; Gevaerts, V. S.; Wienk, M. M.; Janssen, R. A. J. *Angew. Chem., Int. Ed.* **2013**, *52*, 8341−8344.
(15) Kanimozhi, C.; Yaacobi-Gross, N.; Chou, K. W.; Amassian, A.; Anthopoulos, T. D.; Patil, S. *J. Am. Chem. Soc.* **2012**, *134*, 16532−16535.

(16) (a) Huo, L. J.; Zhang, S. Q.; Guo, X.; Xu, F.; Li, Y. F.; Hou, J. H. *Angew. Chem., Int. Ed.* **2011**, *50*, 9697−9702. (b) Huo, L. J.; Hou, J. H.; Zhang, S. Q.; Chen, H. Y.; Yang, Y. *Angew. Chem., Int. Ed.* **2010**, *49*, 1500−1503. (c) Wang, M.; Hu, X. W.; Liu, P.; Li, W.; Gong, X.; Huang, F.; Cao, Y. *J. Am. Chem. Soc.* **2011**, *133*, 9638−9641. (d) Dou, L. T.; Gao, J.; Richard, E.; You, J. B.; Chen, C. C.; Cha, K. C.; He, Y. J.; Li, G.; Yang, Y. *J. Am. Chem. Soc.* **2012**, *134*, 10071−10079. (e) Yang, T. B.; Wang, M.; Duan, C. H.; Hu, X. W.; Huang, L.; Peng, J. B.; Huang, F.; Gong, X. . *Energy Environ. Sci.* **2012**, *5*, 8208−8214. (f) Zhou, J. Y.; Zuo, Y.; Wan, X. J.; Long, G. K.; Zhang, Q.; Ni, W.; Liu, Y. S.; Li, Z.; He, G. R.; Li, C. X.; Kan, B.; Li, M. M.; Chen, Y. S. *J. Am. Chem. Soc.* **2013**, *135*, 8484−8487.

(17) (a) Thomas, S. P.; Love, J. A.; Nguyen, T. Q.; Bazan, G. C. *Adv. Mater.* **2012**, *24*, 3646−3649. (b) Zhang, Y.; Chien, S. C.; Chen, K. S.; Yip, H. L.; Sun, Y.; Davies, J. A.; Chen, F. C.; Jen, A. K. Y. *Chem. Commun.* **2011**, *47*, 11026−11028. (c) Albrecht, S.; Janietz, S.; Schindler, W.; Frisch, J.; Kurpiers, J.; Kniepert, J.; Inal, S.; Pingel, P.; Fostiropoulos, K.; Koch, N.; Neher, D. *J. Am. Chem. Soc.* **2012**, *134*, 14932−14944. (d) Li, Y. X.; Zou, J. Y.; Yip, H. L.; Li, C. Z.; Zhang, Y.; Chueh, C. C.; Intemann, J.; Xu, Y. X.; Liang, P. W.; Chen, Y.; Jen, A. K. Y. *Macromolecules* **2013**, *46*, 5497−5503. (e) Xiao, L.; Liu, B.; Chen, X. W.; Li, Y. F.; Tang, W. J.; Zou, Y. P. *RSC Adv.* **2013**, *3*, 11869−11876.

(18) Duan, C. H.; Cai, W. Z.; Huang, F.; Zhang, J.; Wang, M.; Yang, T. B.; Zhong, C. M.; Gong, X.; Cao, Y. *Macromolecules* **2010**, *43*, 5262−5268.

(19) Beaujuge, P. M.; Tsao, H. N.; Hansen, M. R.; Amb, C. M.; Risko, C.; Subbiah, J.; Choudhury, K. R.; Mavrinskiy, A.; Pisula, W.; Brédas, J. L.; So, F.; Müllen, K.; Reynolds, J. R. *J. Am. Chem. Soc.* **2012**, *134*, 8944−8957.

(20) (a) Henson, Z. B.; Welch, G. C.; van der Poll, T.; Bazan, G. C. *J. Am. Chem. Soc.* **2012**, *134*, 3766−3779. (b) Ying, L.; Hsu, B. Y.; Zhan, H. M.; Welch, G. C.; Zalar, P.; Perez, L. A.; Kramer, E. J.; Nguyen, T. Q.; Heeger, A. J.; Wong, W. Y.; Bazan, G. C. *J. Am. Chem. Soc.* **2011**, *133*, 18538−18541.

(21) (a) Szarko, J. M.; Guo, J. C.; Liang, Y. Y.; Lee, B.; Rolczynski, B. S.; Strzalka, J.; Xu, T.; Loser, S.; Marks, T. J.; Tu, L. P.; Chen, L. X. *Adv. Mater.* **2010**, *22*, 5468−5472. (b) Yiu, A. T.; Beaujuge, P. M.; Lee, O. P.; Woo, C. H.; Toney, M. F.; Fréchet, J. M. *J. Am. Chem. Soc.* **2012**, *134*, 2180−2185.

(22) Yue, W.; Zhao, Y.; Shao, S. Y.; Tian, H. K.; Xie, Z. Y.; Geng, Y. H.; Wang, F. S. *J. Mater. Chem.* **2009**, *19*, 2199−2206.

(23) Davis, R. J.; Lloyd, M. T.; Ferreira, S. R.; Bruzek, M. J.; Watkins, S. E.; Lindell, L.; Sehati, P.; Fahlman, M.; Anthony, J. E.; Hsua, J. W. P. *J. Mater. Chem.* **2011**, *21*, 1721−1729.

(24) Zhu, L.; Cheng, S. Z. D.; Calhoun, B. H.; Ge, Q.; Quirk, R. P.; Thomas, E. L.; Hsiao, B. S.; Yeh, F. J.; Lotz, B. *J. Am. Chem. Soc.* **2000**, *122*, 5957−5967.

(25) Zhang, M.; Yang, C.; Mishra, A. K.; Pisula, W.; Zhou, G.; Schmaltz, B.; Baumgarten, M.; Müllen, K. *Chem. Commun.* **2007**, *17*, 1704−1706.

(26) Mei, J. G.; Kim, D. H.; Ayzner, A. L.; Toney, M. F.; Bao, Z. N. *J. Am. Chem. Soc.* **2011**, *133*, 20130−20133.

(27) Becke, A. D. *J. Chem. Phys.* **1993**, *98*, 5648−5652.

(28) Dewar, M. J. S.; Zoebisch, E. G.; Healy, E. F.; Stewart, J. J. P. *J. Am. Chem. Soc.* **1985**, *107*, 3902−3909.

(29) (a) Tsao, H. N.; Cho, D. M.; Park, I.; Hansen, M. R.; Mavrinskiy, A.; Yoon, D. Y.; Graf, R.; Pisula, W.; Spiess, H. W.; Müllen, K. *J. Am. Chem. Soc.* **2011**, *133*, 2605−2612. (b) Osaka, I.; Zhang, R.; Sauvé, G.; Smilgies, D. M.; Kowalewski, T.; McCullough, R. D. *J. Am. Chem. Soc.* **2009**, *131*, 2521−2529.

(30) Rose, A. *Phys. Rev.* **1955**, *97*, 1538−1544.

(31) (a) Kreouzis, T.; Baldwin, R. J.; Shkunov, M.; McCulloch, I.; Heeney, M.; Zhang, W. *Appl. Phys. Lett.* **2005**, *87*, 172110. (b) Murgatroyd, P. N. *J. Phys. D: Appl. Phys.* **1970**, *3*, 151−156.

(32) Huang, F.; Wu, H. B.; Wang, D. L.; Yang, W.; Cao, Y. *Chem. Mater.* **2004**, *16*, 708−716.

(33) Lee, J. K.; Ma, W. L.; Brabec, C. J.; Yuen, J.; Moon, J. S.; Kim, J. Y.; Lee, K.; Bazan, G. C.; Heeger, A. J. *J. Am. Chem. Soc.* **2008**, *130*, 3619−3623.

(34) He, Y. J.; Chen, H. Y.; Hou, J. H.; Li, Y. F. *J. Am. Chem. Soc.* **2010**, *132*, 1377−1382.

(35) Roncali, J. *Acc. Chem. Res.* **2009**, *42*, 1719−1730.